Supplementary Information for

Continuous Flow Synthesis of MOF/Nanocarbon Composites

Almond Lau,[a] Ji Feng,[*a] Stefan H. Bossmann,[b,c] Dymphna Sebastian,[b,c] Christopher M. Sorensen,[b,d] and Igor V. Novosselov[*a]

[a.]Department of Mechanical Engineering and Institute for Nano-Engineered Systems University of Washington, 3900 E Stevens Way NE, Seattle, WA 98195, United States
E-mail: jfeng003@uw.edu, ivn@uw.edu
[b.]HydroGraph Clean Power, Inc, 809H Levee Drive, Manhattan, KS 66502, USA
[c.] Department of Cancer Biology, University of Kansas Medical School, Kansas City, KS 66160, USA
[d.] Department of Physics, Kansas State University, Manhattan, KS 66506, USA

Materials

All obtained chemical products were used in their supplied condition without additional purification. Zirconyl chloride octahydrate ($ZrOCl_2 \cdot 8H_2O$, 98%), 2-aminoterephthalic acid (NH_2-BDC, 99%), and acetic acid (AA, ≥99.7%) were purchased from Sigma-Aldrich, Darmstadt, Germany and dissolved in N,N-dimethylformamide (DMF, ≥99.80%, Carolina Chemical, Charlotte, NC, USA).

Carboxyl-modified reactive graphene aggregate (CGA) was provided by Hydrograph Clean Power, Inc. The CGA was obtained via functionalization of FGA-1 with 4-Chloromethylbenzoic Acid (4-CMB Acid). FGA-1 (20.0 g) was dispersed in tert-butyl acetate (300 mL) in a 500 mL round-bottom flask equipped with a heating mantle and reflux condenser under an argon atmosphere. The suspension was heated to 40 °C with continuous stirring. Sodium azide (NaN_3, 3.60 g, 0.055 mol) was added, followed by 4-chloromethylbenzoic acid ($C_8H_7ClO_2$, 9.40 g, 0.055 mol). The reaction mixture was stirred at 40 °C for 60 min. The temperature was subsequently increased to 80 °C, and stirring was continued for an additional 120 min. After completion of the reaction, the mixture was

allowed to cool to room temperature. The modified FGA-1 was isolated by vacuum filtration and washed three times with cold tert-butyl acetate (3 × 10 mL, 0 °C). The material was dried in an air oven at 50 °C overnight. Residual inorganic salts (e.g., NaCl) and organic salts were removed by treating the solid with 95% methanol in water, followed by thorough washing with deionized (DI) water. The product was again collected by filtration, washed three times with DI water (3 × 15 mL), and dried in an air oven at 80 °C overnight to afford the functionalized FGA-1 as a black solid (Yield: 18.4 ± 1.2 g). FTIR confirmed successful surface modification (Figure S5).

CGA was added to the precursor solutions in varying weight percentages of the UiO-66-NH_2 estimated product yield to form UiO-66-NH_2/CGA composites with 0, 5, 10, 20, and 30 wt% CGA, named UiO-66-NH_2, U66N/CGA5, U66N/CGA10, U66N/CGA20, and U66N/CGA30, respectively. Carbon dioxide (CO_2, 99.5%, Linde, Danbury, CT, USA) was used in reactor operation and ethanol (200 proof, Decon Labs, Inc., King of Prussia, PA, USA) was used in sample washing.

Reactor Setup

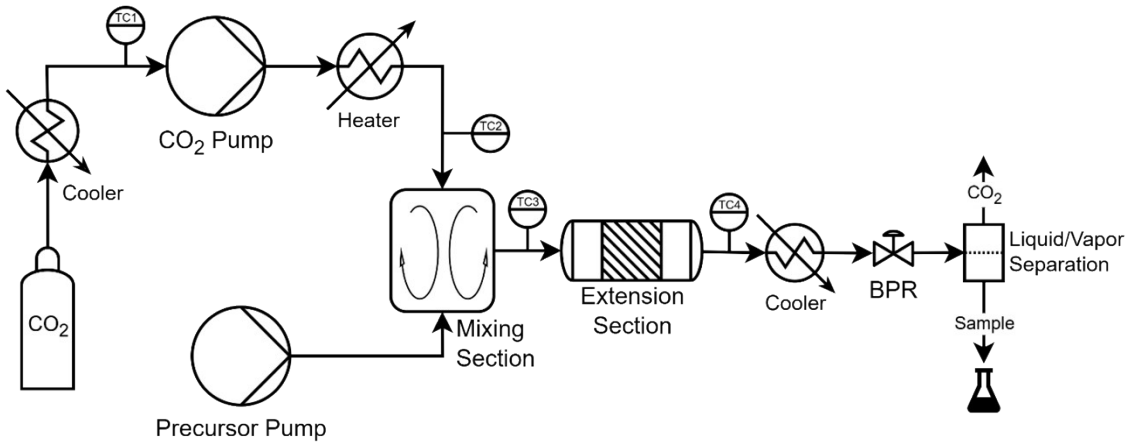

Figure S1. Process diagram of the $scCO_2$ continuous flow reactor setup utilizing a countercurrent mixing section and an extension section. Thermocouples (TCs) are numbered and placed throughout the reactor to monitor temperatures, while the back pressure regulator (BPR) maintains system pressure.

The residence time was estimated by linearly fitting and extrapolating available solubility [1] and density [2] data at ~10 MPa to the 140 °C reactor temperature (assuming the extension temperature is the average reactor temperature). To simplify the calculation, the precursor was assumed to be completely DMF. In doing so, the solubility of CO_2 in the DMF-rich liquid phase is ~0.3 mol mol^{-1} and the solubility of DMF in the CO_2 rich gas-like supercritical phase is assumed to be negligible based off lower temperature data.[3] Using the molar flow rates of each constituent of each phase and estimated densities (where CO_2 densities were obtained from the NIST database [4]), we calculated the volumetric flow rate of each phase and divided the reactor volume (~155.5 mL including the mixing section) by the sum of the volumetric flow rates to obtain a residence time of ~1.2 min.

Synthesis and Activation

$ZrOCl_2 \cdot 8H_2O$ and NH_2-BDC were dissolved in AA/DMF (50/50 vol%) to form the 0.5 M precursor solution for UiO-66-NH_2. 0.175-1.05 g L^{-1} of CGA were dispersed in the precursor solution for U66N/CGA5, U66N/CGA10, U66N/CGA20, and U66N/CGA30. These precursor solutions were used for synthesis of their corresponding materials in the $scCO_2$ reactor. After collection, the materials were distributed into 50 mL polypropylene tubes and centrifuged (Eppendorf 5430 Centrifuge) at 7830 rpm for 8 min. The supernatant was removed, and the solid product was washed twice with DMF and twice with ethanol before drying overnight in an oven at 140 °C. After weighing the final product, the weight percentage of CGA in each sample were determined to be 5.5%, 11%, 22%, and 33% for U66N/CGA5, U66N/CGA10, U66N/CGA20, and U66N/CGA30, respectively.

MOF/Graphene Synthesis Methods

Table S1. Comparison of MOF/graphene composites synthesized by published batch methods and by our $scCO_2$ continuous flow method, including reaction time, graphene surface modifications (if specified), composite morphology, and specific surface area (SSA). G = graphene, GO = graphene oxide, rGO = reduced graphene oxide.

MOF/Graphene (Ref.)	Application	Method	Time (h)	Surface Modification	Morphology	SSA ($m^2\ g^{-1}$)
UiO-66-NH_2/G ([5])	CO_2 reduction	Solvothermal (microwave)	0.67	--	MOF nanocrystals dispersedly covering larger GO sheets	791
UiO-66(-NH_2)/ rGO ([6])	CO_2 reduction	Mix + hydrothermal treatment	3	--	MOF nanocrystals densely covering larger GO sheets	289, 504
UiO-66-NH_2/rGO ([7])	H_2 production	Mix + hydrothermal treatment	12	--	MOF nanocrystals wrapped in GO sheets	--
MIL-125-NH_2(Ti)/ rGO ([8])	Dye degradation	Solvothermal	48	Hummers method	MOF nanocrystals densely covering larger rGO sheets	750
MOF-801/GO ([9])	Dye degradation	Solvothermal	6	Hummers method	MOF nanocrystals densely covering larger GO sheets	517
UiO-66-NH_2/GO ([10])	Antibiotic sensing	Mechanochemical	1.33	Chlorination (with PCl_5)	MOF nanocrystals dispersedly covering larger GO micro-sheets	--
MIL-53(Fe)/rGO ([11])	Dye degradation	Solvothermal	72	Hummers method	MOF microcrystals with rGO micro-sheets anchored on surface	--
UiO-66-NH_2/rGO ([12])	Organic oxidation	Solvothermal	48	Pyrene	MOF nanocrystals densely covering larger rGO sheets	750
HKUST-1/GO ([13])	--	Pickering emulsion	1	Hummers method	MOF nanocrystals and micro-rods dispersedly covering larger GO micro-sheets	740-900
UiO-66-NH_2/CGA (This Work)	--	$ScCO_2$ continuous flow	0.02	Carboxyl	MOF nano-shell around nano-graphene aggregates	795-1011

Characterization of CGA

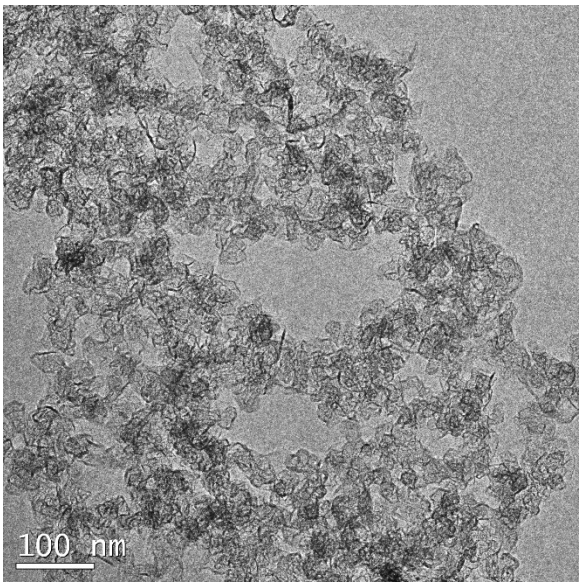

Figure S2. TEM image of CGA.

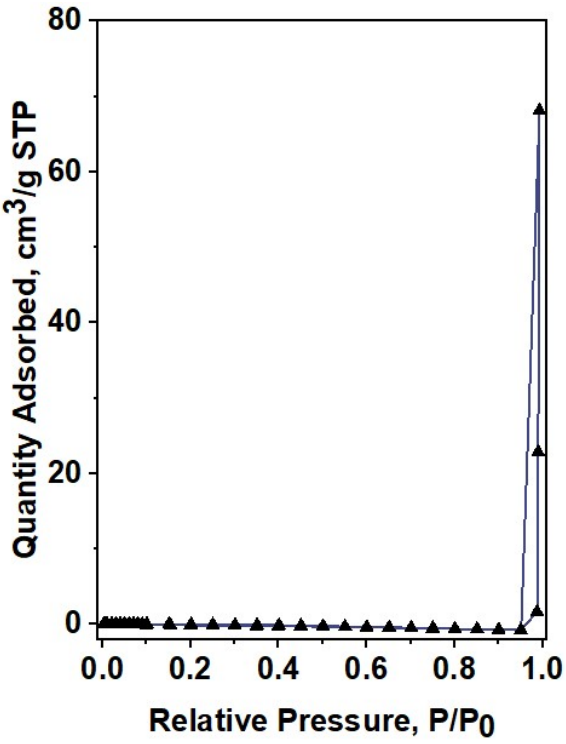

Figure S3. N_2 adsorption and desorption isotherm of CGA.

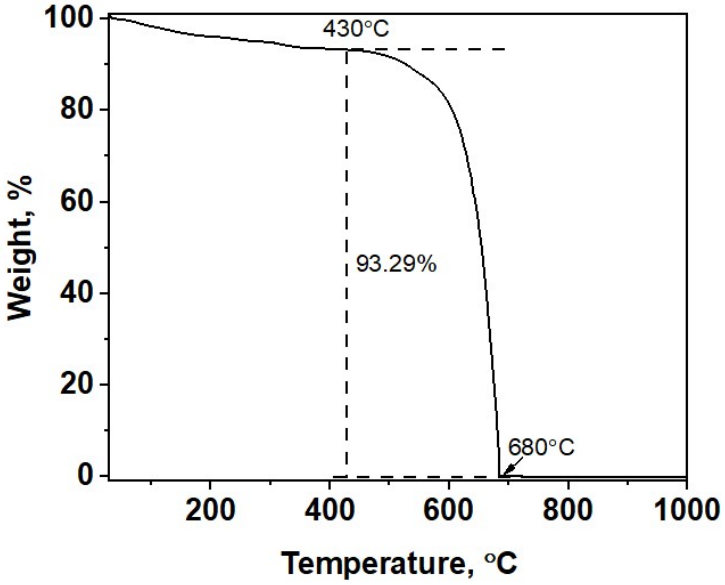

Figure S4. TGA curve of CGA.

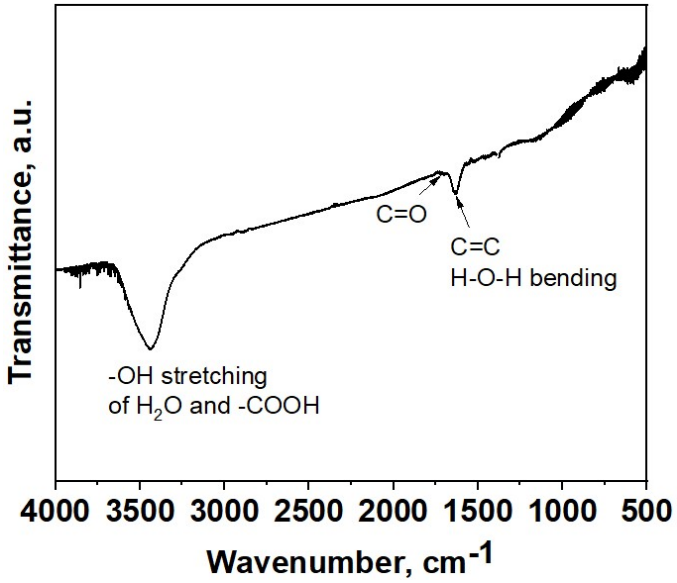

Figure S5. FTIR of CGA.

Characterization of U66N/CGA

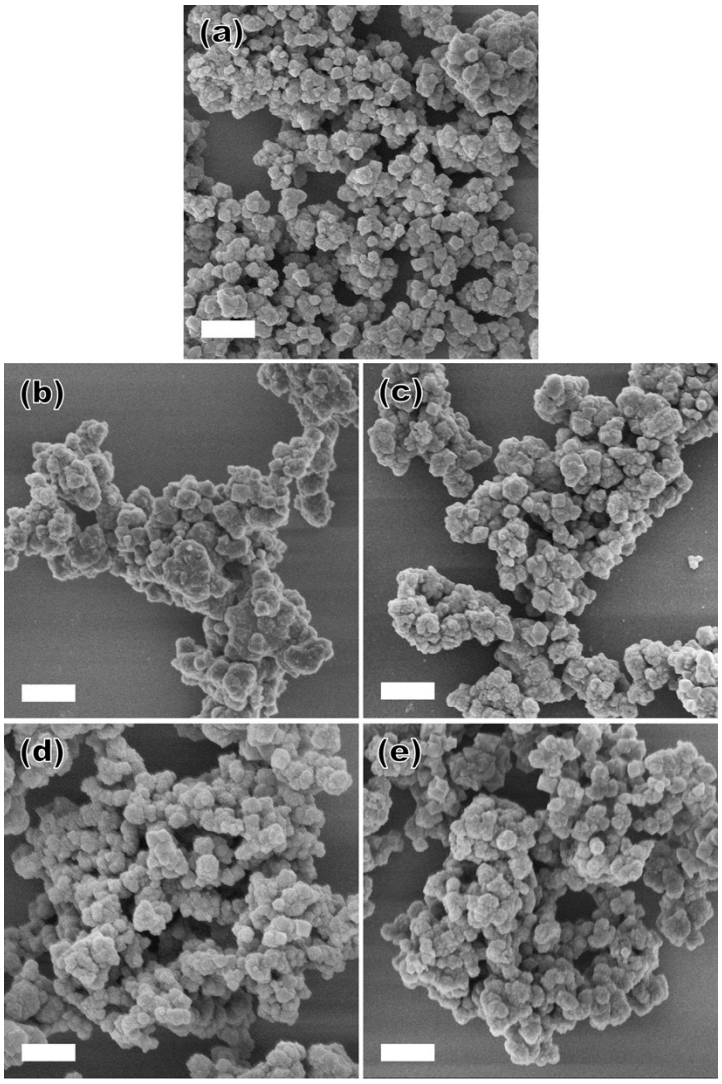

Figure S6. SEM images of UiO-66-NH_2 with CGA content of 0 % (a), 5 % (b), 10 % (c), 20 % (d), and 30 % (e). The scale bars in all figures are 500 nm.

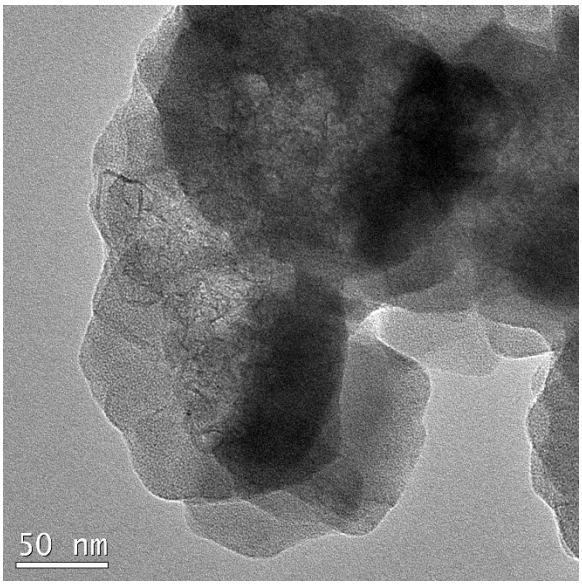

Figure S7. TEM image of U66N/CGA10.

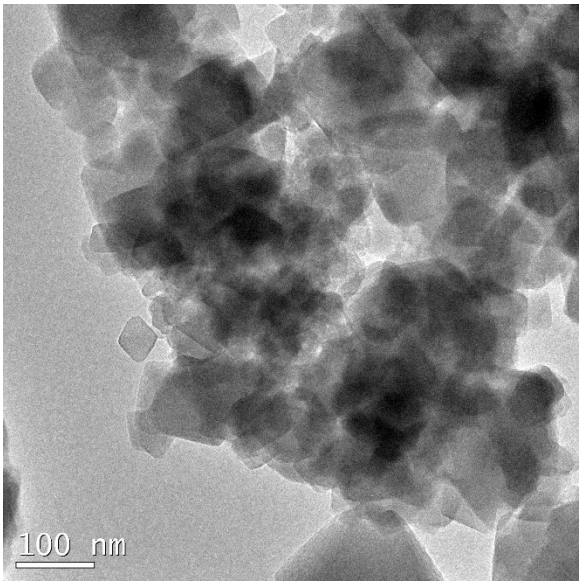

Figure S8. TEM image of U66N/CGA5.

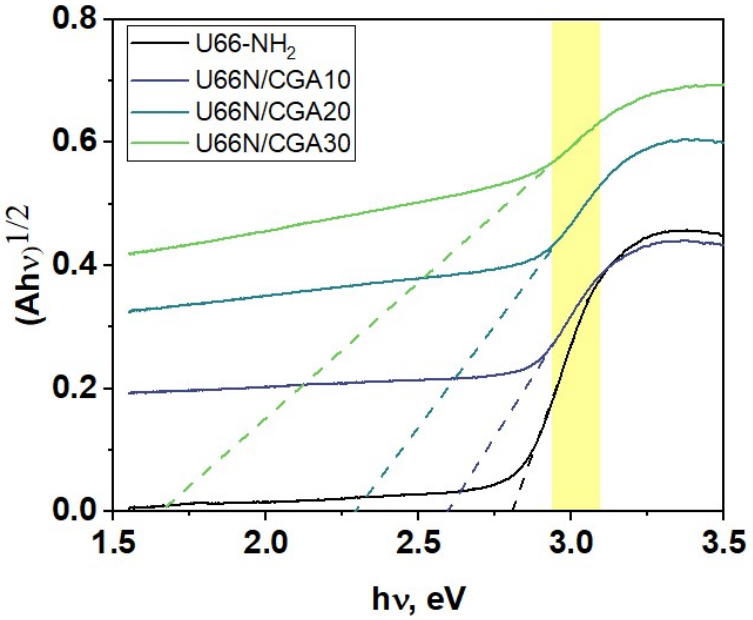

Figure S9. Tauc plot of UiO-66-NH_2 and U66N/CGA. Linear fit for all samples were performed in the window of 2.94-3.10 eV (yellow box).

References

1. H. S. Byun, N. H. Kim and C. Kwak, *Fluid Phase Equilib.*, 2003, **208**, 53-68.
2. A. Zúñiga-Moreno and L. A. Galicia-Luna, *J. Chem. Eng. Data*, 2005, **50**, 1224-1233.
3. K. Liu, L. Zheng, Y. Wang, L. Hou and Y. Ma, ed. P.J. Linstrom and W.G. Mallard, *2011 International Conference on Materials for Renewable Energy & Environment*, 2011, **2**, 1478-1482.
4. E. W. Lemmon, I. H. Bell, M. L. Huber, and M. O. McLinden, in *NIST Chemistry WebBook, NIST Standard Reference Database Number 69*, National Institute of Standards and Technology, Gaithersburg MD, 2026.
5. X. Wang, X. Zhao, D. Zhang, G. Li and H. Li, *Appl. Catal., B*, 2018, **228**, 47-53.
6. X. Zhao, M. Xu, X. Song, W. Zhou, X. Liu, Y. Yan and P. Huo, *Chem. Eng. J.*, 2022, **437**, 135210.
7. Y. Wang, Y. Yu, R. Li, H. Liu, W. Zhang, L. Ling, W. Duan and B. Liu, *J. Mater. Chem. A*, 2017, **5**, 20136-20140.
8. L. Huang and B. Liu, *RSC Adv.*, 2016, **6**, 17873-17879.
9. Z. Wu, Z. Chen, J. Chen, X. Ning, P. Chen, H. Jiang and H. Qiu, *Environ. Sci.: Nano*, 2022, **9**, 4609-4618.
10. D. Bigdelifam and M. Hashemi, *ACS Omega*, 2025, **10**, 16184-16193.
11. Y. Zhang, G. Li, H. Lu, Q. Lv and Z. Sun, *RSC Adv.*, 2014, **4**, 7594.
12. J. Xu, S. He, H. Zhang, J. Huang, H. Lin, X. Wang and J. Long, *J. Mater. Chem. A*, 2015, **3**, 24261-24271.
13. Z. Bian, J. Xu, S. Zhang, X. Zhu, H. Liu and J. Hu, *Langmuir*, 2015, **31**, 7410-7417.